



# Simulated body-fluid tests and electrochemical investigations on biocompatibility of metallic glasses

C.H. Lin <sup>a</sup>, C.H. Huang <sup>b</sup>, J.F. Chuang <sup>a</sup>, H.C. Lee <sup>a</sup>, M.C. Liu <sup>b</sup>, X.H. Du <sup>b</sup>, J.C. Huang <sup>b,\*</sup>, J.S.C. Jang <sup>c</sup>, C.H. Chen <sup>d,e</sup>

<sup>a</sup> Department of Mechanical and Electro-Mechanical Engineering, National Sun Yat-Sen University, Kaohsiung, Taiwan, ROC

<sup>b</sup> Department of Materials and Optoelectronic Science, Center for Nanoscience and Nanotechnology, National Sun Yat-Sen University, Kaohsiung, Taiwan, ROC

<sup>c</sup> Department of Mechanical Engineering, Institute of Materials Science and Engineering, National Central University, Chung-Li, Taiwan, ROC

<sup>d</sup> Departments of Orthopedics and Orthopedic Research Center, College of Medicine, Kaohsiung Medical University, Kaohsiung, Taiwan, ROC

<sup>e</sup> Department of Orthopedics, Kaohsiung Medical University Hospital, Kaohsiung Medical University, Kaohsiung, Taiwan, ROC

## ARTICLE INFO

### Article history:

Received 13 April 2012

Received in revised form 10 July 2012

Accepted 28 July 2012

Available online 3 August 2012

### Keywords:

Metallic glasses

Simulation body-fluid

Corrosion resistance

Bio-toxicity

Electrochemical stability

## ABSTRACT

This paper presents the in-vitro and electrochemical investigations of four metallic glasses (MGs) for finding potential MG-based bio-materials. The simulation body-fluid Hanks solution is utilized for testing the corrosion resistance of MGs, and microorganisms of *Escherichia coli* are used in testing the bio-toxicity. In addition, a simple cyclic voltammetry method is used for rapid verification of the potential electrochemical responses. It is found that the Zr-based MG can sustain in the body-fluid, exhibiting the best corrosion resistance and electrochemical stability. The microbiologic test shows that *E. coli* can grow on the surface of the Zr-based metallic glass, confirming the low cell toxicity of this Zr-based MG.

© 2012 Elsevier B.V. All rights reserved.

## 1. Introduction

During the last decades, scientists have put substantial efforts on finding better materials for medical implants and other clinical applications. Biocompatibility of the implanted materials is one of the most important issues needed to be considered. The implanted materials directly contacting tissues must avoid any toxic, irritating, inflammatory, allergic, or carcinogenic action [1–4]. Nowadays, pure titanium is the most popular metal for producing long-term implantable devices due to its excellent biocompatibility. However, the low strength and low hardness of commercial pure titanium (CP Ti, typically ~300–500 MPa for tensile strength and ~1 GPa for hardness) is of concern for some clinical applications. In this regard, a number of titanium alloys were developed for biomedical applications [5,6]. The composition and microstructure, especially the grain boundaries, of Ti alloy materials are much more complex in comparison with CP Ti. The high ionic strength, warm temperature and a great number of microorganisms in human body can cause biodegradation of the implant materials [7], such that the patient may be exposed to corrosive products and suffered from unwanted bio-reactions [8]. For example, highly corrosive materials in body may release cytotoxic ions and cause cell apoptosis and necrosis [9]. Therefore, some metallic glassy materials were studied

for biomedical applications in the recent years since there is no grain boundary in the amorphous structure of metallic glasses (MGs). Some undesired electrochemical corrosion preferentially associated with grain boundaries might be suppressed or eliminated while using MGs with amorphous structures [10].

Metallic glasses have a unique atomic structure, so they do not contain the microstructural defects such as vacancies, dislocations, twins, or grain boundaries. Metallic glasses usually have more promising corrosion-resistant properties [11,12], high mechanical strength in the range of 800–3000 MPa [13], and superplastic processing capabilities within the supercooled liquid temperature region above the glass transition temperature [14], making them highly feasible for biomedical implant applications [10]. Moreover, metallic glasses usually have lower Young's modulus [13,15,16] in comparison with typical crystalline metal materials such that the stress shielding effect can be reduced for implant applications. Among the massive MGs developed so far, the Fe-, Zr-, and Mg-based metallic glass alloys are most matured and commercially economic. Bulk metallic glasses (BMGs) of the Ni-, Cu-, or Al-based alloys contain abundant harmful Ni, Cu or Al as their matrix elements. The Pd- or Au-based BMGs are unlikely to be accepted for their high cost. Ti-based alloys are still difficult to be cast into large size for bio-implant. Although some of the current Fe-, Zr-, and Mg-based BMGs still contain various amounts of undesired Ni, Cu or Al, the contents of the latter elements are always present as the minor constituents. Preliminary biocompatibility tests showed acceptable responses [17–20].

\* Corresponding author at: 70 Lian-Hai Road, Kaohsiung, Taiwan, ROC. Tel.: +886 7 525 2000x4063; fax: +886 7 525 4099.

E-mail address: [jacobc@mail.nsysu.edu.tw](mailto:jacobc@mail.nsysu.edu.tw) (J.C. Huang).

In this study, we attempt to compare the bio-compatibility of some representative metallic glassy materials by simple in-vitro tests. Simulation body-fluid immersion is used to test the corrosion resistance of four self-made metallic glasses. A novel electrochemical test by measuring the cyclic voltammetry response of the metallic glasses in the simulation body-fluid is developed. With this approach, analyzing the electrochemical response of the metallic glasses in body can be achieved in a short time. The long-term electrochemical corrosion response of the MGs in human body-fluid can be predicted without long-term and continuous observation. Moreover, the potential elements in the MGs that cause the electrochemical corrosion can also be briefly identified. The biotoxicity of the MGs is finally tested by culturing *E. coli* on the MG surfaces. The methods developed in the present study provide a simple and fast way to screen potential metallic glasses for bio-applications.

## 2. Materials and methods

Four metallic glass ribbons, with nominal compositions of  $\text{Mg}_{65}\text{Cu}_{25}\text{Gd}_{10}$ ,  $\text{Mg}_{67}\text{Cu}_{25}\text{Y}_8$ ,  $\text{Zr}_{61}\text{Cu}_{17.5}\text{Ni}_{10}\text{Al}_{7.5}\text{Si}_4$  and  $\text{Fe}_{70}\text{B}_{20}\text{Si}_{10}$  (all in atomic percent) were fabricated by melt spinning, starting with pure elements of Mg (99.99 wt.%), Cu (99.999 wt.%), Gd (99.9 wt.%), Y (99.9 wt.%), Zr (99.9 wt.%), Ni (99.9 wt.%), Al (99.99 wt.%), Si (99.999 wt.%), Fe (99.99 at.%), and B (99.9 wt.%). The amorphous nature and compositions of the as-melt-spun ribbons were verified X-ray diffractometry (XRD) and scanning electronic microscopy with energy dispersive spectrometry (SEM/EDS). The XRD was performed with a  $\text{Cu K}\alpha$  radiation ( $\lambda = 1.5406 \text{ \AA}$ ) equipped with a 0.02 mm graphite monochromator (D5000, Siemens, German), operated at 40 kV and 30 mA. The ranges of the diffraction angle ( $2\theta$ ) were from  $20^\circ$  to  $80^\circ$  with a scan rate of  $0.1^\circ$  for 5 s. SETARAM DSC 131 differential scanning calorimeter (DSC) at a constant heating rate of 0.33 K/s (or 20 K/min) was used for evaluating the thermal properties of the produced MGs.

The MG ribbons of around 100  $\mu\text{m}$  in thickness were cut into small pieces with the size around  $5 \text{ mm} \times 5 \text{ mm}$  and  $5 \text{ mm} \times 10 \text{ mm}$  for simulation body-fluid tests and *E. coli* (DH5 $\alpha$ ) biotoxicity tests, respectively. The simulation body-fluid test of these amorphous metallic sheets were characterized by immersing these MGs into a 10-mL physiological isotonic solutions (the Hank's solution, pH: 6.5 and 2.0) at  $37^\circ\text{C}$ . The typical Hank's solution is composed of 0.137 M of NaCl, 5.4 mM of KCl, 0.25 mM of  $\text{Na}_2\text{HPO}_4$ , 0.44 mM of  $\text{KH}_2\text{PO}_4$ , 1.3 mM of  $\text{CaCl}_2$ , 1.0 mM of  $\text{MgSO}_4$ , 4.2 mM of  $\text{NaHCO}_3$ . Instead of using the common simulation body-fluid of Kokubo's solution, Hank's balanced salt solution was used for in-vitro tests for the biocompatibility of biomaterials due to the lower concentration of  $\text{Cl}^-$  ion (148.8 mM for Kokubo's solution, 143.7 mM for Hank's solution and 103.3 mM for human plasma). As reported by the previous studies, the concentration of chlorine ion is the major factor which

causes the corrosion of MG metals such that the Hank's solution was used in the present study [21,22]. The pH values were verified by the pH meter. The surface morphologies of surface of the samples were examined by optical microscopy (OM) and SEM.

Biotoxicity tests of the MGs passing the simulation body-fluid tests were then conducted in according to a standard in-vitro test procedure used with *E. coli* (DH5 $\alpha$ ,  $0.5 \times 1-3 \mu\text{m}$ ) [23,24]. Cells were cultured in the Luria-Bertani (LB) agar plate at  $37^\circ\text{C}$  with various culture conditions. The 2  $\mu\text{L}$  DH5 $\alpha$  medium (composed of tryptophan, yeast extract and NaCl) was used for the in-vitro test and the specimens were cultured in the LB plate for 16 h. It is noted that the concentration of DH5 $\alpha$  medium was around  $1.3 \times 10^9$  cells/mL. The growth of DH5 $\alpha$  and the morphology of MG surfaces were observed and characterized by SEM. Electrochemical tests of MGs were performed to analyze the behavior of transferred electrons between the solution and MGs. The potential corrosion reactions between the MGs and simulation solution were characterized using a standard cyclic voltammetry with the scanning potential from 1 V to  $-1$  V.

## 3. Results and discussion

The four MG ribbons were first examined by SEM/EDS for assurance of their alloy compositions. The current melt spinning can fabricate smooth ribbons with highly controlled and precise compositions, all very close to the set element contents. Then, they were checked by XRD and DSC for confirming their amorphous structure and glass transition, as shown in Fig. 1. As presented in Fig. 1(a), only a broad diffused amorphous hump was observed in the XRD patterns, confirming the amorphous structure of the MG materials used in the present study. The glass transition and crystallization temperatures determined by DSC for these four MGs are around 420 and 480 K for  $\text{Mg}_{65}\text{Cu}_{25}\text{Gd}_{10}$ , 410 and 465 K for  $\text{Mg}_{67}\text{Cu}_{25}\text{Y}_8$ , 663 and 723 K for  $\text{Zr}_{61}\text{Cu}_{17.5}\text{Ni}_{10}\text{Al}_{7.5}\text{Si}_4$ , and 740 and 780 K for  $\text{Fe}_{70}\text{B}_{20}\text{Si}_{10}$ , respectively.

The compressive strength and hardness of the four MGs are measured, and the data are listed in Table 1, in comparison with those for the CP Ti. It can be seen that the strength of the MGs are typically in the range of 800 to 2500 MPa, considerably higher than the 300–500 MPa of CP Ti. The same is for the high hardness for MGs, 2.5 to 7 GPa, much higher than the  $\sim 1$  GPa for CP Ti. As presented below, the Zr-based MG appears to most promising, and the strength and hardness show great improvement with respect to CP Ti.

Fig. 2 presents the results for immersing the MGs into the Hank's solutions with two different pH values of 2.0 and 6.5. Note that the solution with the pH value of 2.0 was adjusted by adding hydrochloric acid into the bath to simulate the strongest acidity in human body. The pH level of 2.0 might be the most extreme condition that most implant materials might not encounter, but can greatly shorten the

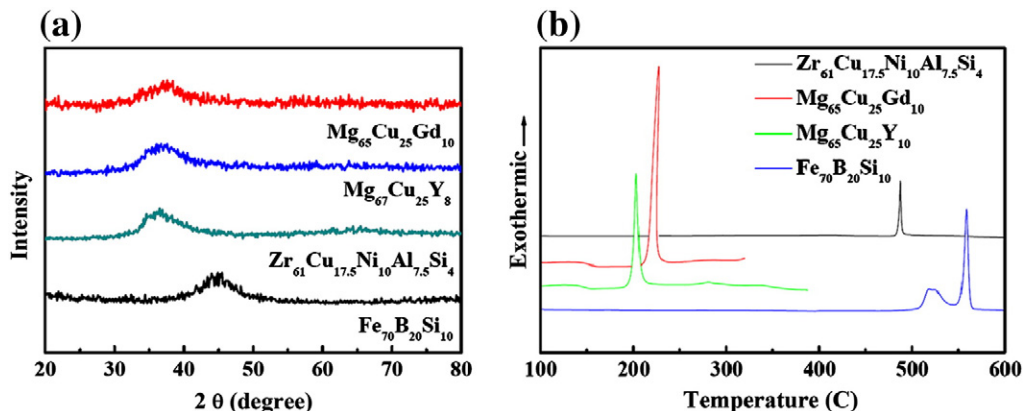
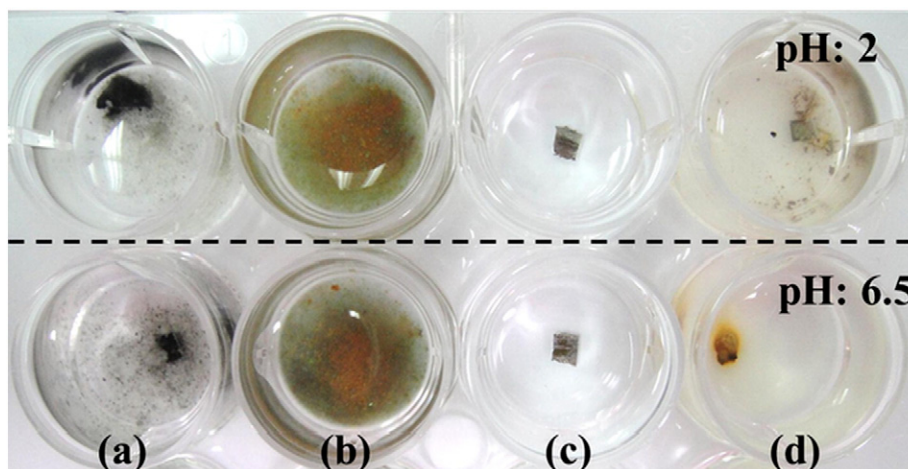


Fig. 1. (a) XRD scans and (b) DSC scans for the four MG ribbons.

**Table 1**

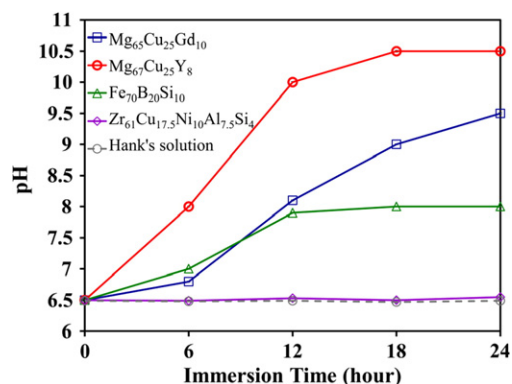
Comparison of the compressive flow strength and hardness of the five materials under consideration.

	CP Ti	Mg <sub>65</sub> Cu <sub>25</sub> Gd <sub>10</sub>	Mg <sub>67</sub> Cu <sub>25</sub> Y <sub>8</sub>	Zr <sub>61</sub> Cu <sub>17.5</sub> Ni <sub>10</sub> Al <sub>7.5</sub> Si <sub>4</sub>	Fe <sub>70</sub> B <sub>20</sub> Si <sub>10</sub>
Strength, MPa	~400	~800	~800	~1800	~2500
Hardness, GPa	~1	~2.5	~2.5	~5	~7

**Fig. 2.** The corrosion response for the four MGs immersed in Hank's solution for 24 h under two pH levels of 2.0 and 6.5: (a) Mg<sub>65</sub>Cu<sub>25</sub>Gd<sub>10</sub>, (b) Mg<sub>67</sub>Cu<sub>25</sub>Y<sub>8</sub>, (c) Zr<sub>61</sub>Cu<sub>17.5</sub>Ni<sub>10</sub>Al<sub>7.5</sub>Si<sub>4</sub>, and (d) Fe<sub>70</sub>B<sub>20</sub>Si<sub>10</sub>.

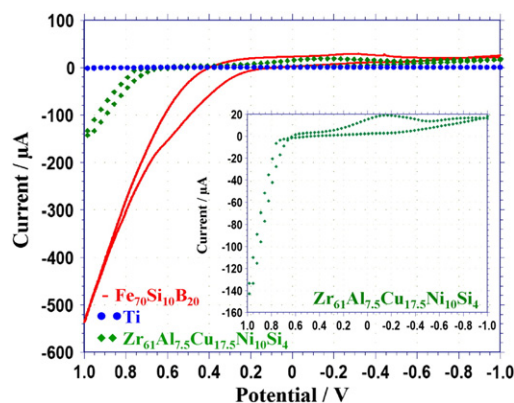
observation time for possible corrosion reactions. In contrast, the pH level of 6.5 would be the common human body environment that of more concern. It is postulated that the immersion corrosion degree in the pH = 2.0 Hank's solution for 24 h might have corresponded to that in the pH = 6.5 Hank's solution for months or years. The Mg- and Fe-based MG materials showed severe corrosion in both baths (pH = 2.0 and 6.5) after 24 h of immersion, but the Zr-based MG remained its morphology without significant corrosive phenomenon. It is clear that the Zr<sub>61</sub>Cu<sub>17.5</sub>Ni<sub>10</sub>Al<sub>7.5</sub>Si<sub>4</sub> metallic glassy alloy possesses a much higher corrosion resistance and is considered to pass the simulation body-fluid immersion test.

When the immersed MGs undergo corrosion or degradation, the dissolved metal ions would induce hydrolysis and increase the Hank's solution pH level. Fig. 3 presents the variation of the measured pH values with increasing immersion time in the Hank's solution with initial pH value of 6.5. Here, only the variation for the Hank's solution

**Fig. 3.** Variations of the pH values as a function of immersion time for the Hank's solution itself, as well as the Hank's solution immersed with the four MGs. Only the variation for initial pH = 6.5 is shown.

with initial pH = 6.5 is shown. For the case of initial pH = 2.0, the solution pH level was not changed significantly due to the strong initial acidity. Results showed that the Mg- and Fe-based MGs all show apparent increase in pH values, suggesting degradation in the Hank's solution. It is also noted that rapid hydrogen evolution has occurred for these MGs. By contrast, the pH values for the bath immersed with Zr-based MG remained the same, indicating that there was basically no metal ion dissolution in the Hank's solution. In this regard, this Zr-based MG is promising in corrosion screening, and is chosen for further in-vitro cell culture tests.

The cyclic voltammetry test results for better behaved Zr- and Fe-based MGs are shown in Fig. 4. A standard pure Ti screw was also measured as the standard for this test. The result illustrates that the standard pure Ti remains no redox peak and the charge current induced by pure Ti is also small, while the Fe<sub>70</sub>B<sub>20</sub>Si<sub>10</sub> metallic glass exhibits strong redox reaction from 0 V to 1 V. Alternatively, the Zr-based metallic glassy alloy obviously has much lower current

**Fig. 4.** The comparison of cyclic voltammograms for various MGs and pure Ti in Hank's solution. In the inset shows the cyclic voltammograms of Zr<sub>61</sub>Cu<sub>17.5</sub>Ni<sub>10</sub>Al<sub>7.5</sub>Si<sub>4</sub> only.



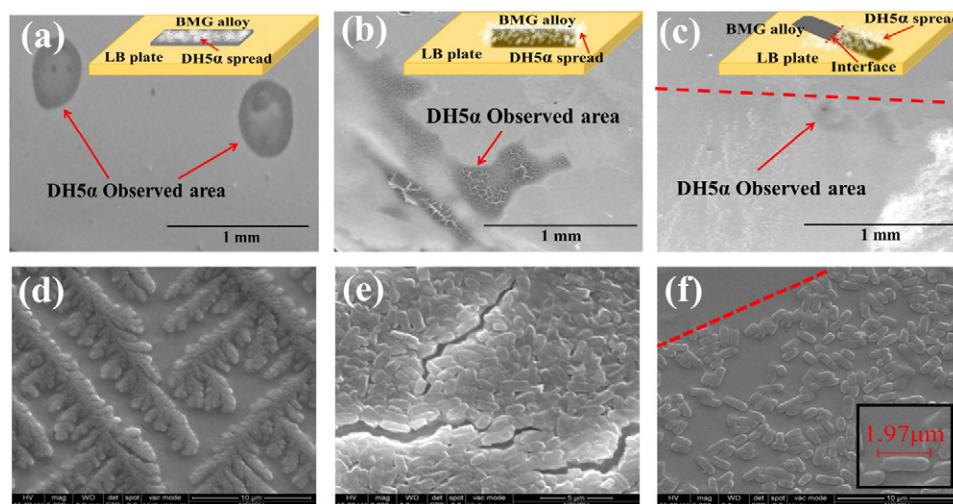


**Fig. 5.** SEM micrographs of the Zr-based MG surface after culturing DH5α for 16 h via the condition of (a) MG surface without the LB plate, (b) MG surface with thin LB plate, (c) MG with half insertion into the LB plate. (d)–(f) are the enlarged views of (a)–(c).

response compared to the current obtained with the Fe-based glassy alloy. However, in comparison with the standard pure Ti, the induced current response of the Zr-based MG is still slightly higher at high potential levels. The inset in Fig. 4 shows an enlarged CV (current–voltage) curve for the Zr-based MG. Through comparison with the CV response curves obtained individually from pure elements of Zr, Cu, Ni, Al and Si, the redox hump, shown in the insert of Fig. 4 for  $\text{Zr}_{61}\text{Cu}_{17.5}\text{Ni}_{10}\text{Al}_{7.5}\text{Si}_4$ , between  $-0.4$  V and  $0$  V is considered to be caused by the minor oxidation of Al or Cu in the Hank's solution. The Zr-based metallic glassy alloy shows the best potential among the four MGs for the further biocompatibility research in the human body.

Fig. 5 shows the SEM images of the Zr-based MG surface morphology after DH5α subculture for 16 h. The test conditions, as presented in the insets of Fig. 5(a)–(c), were designed to examine the biocompatibility of Zr-based MG, including the biotoxicity and cell induction property for DH5α. Note that the control group for the biotoxicity assay was the case for culturing DH5α using pure culture medium without MG sample. By comparing the growth behavior of DH5α for the control group and the designed tests, the short-term biotoxicity of different MGs could be simply evaluated. For the condition of Fig. 5(a), DH5α was spread onto the MG surface without covering the LB plate. The bacteria were directly contacted with the MG surface to test the immediate biotoxicity of the MG. For Fig. 5(b), DH5α was spread on the MG surface with a thin layer of LB plate, testing the short-term effect for the MG response. For Fig. 5(c), DH5α was first spread on the LB plate then the MG was half inserted into the culture medium, exposing half of clean MG surface above the LB agar. This condition created an exact interface between the spread DH5α and clean MG surface, which was designed to observe if DH5α could grow uphill to the MG surface without culture medium. The cell induction property of this MG could be roughly estimated. The cell density shown in Fig. 5(a) is a bit lower than the bacteria density in Fig. 5(b), since there was no medium supplied for the case in Fig. 5(a). There are also water-mark patterns formed for the spread DH5α sample after drying, as seen in Fig. 5(a), due to the hydrophobicity of the MG surface.

Fig. 5(d)–(f) presents the close-up views for the cases of Fig. 5(a)–(c), respectively. The close-up SEM view in Fig. 5(d) shows that DH5α gathered and formed a packed pattern with the shape similar to the dry pattern of a liquid drop on a solid surface. In addition, it is also noticed the size of DH5α shrank slightly due to the lacking of water supply, resulting in the morphology change of the cultured cells. The DH5α growth pattern in Fig. 5(b) appears to be identical to the pattern of DH5α growth on pure LB agar without MG. A

dense growth pattern and round-shaped DH5α can be observed in Fig. 5(b) or Fig. 5(e). Finally, there is a distinct cell-growth line observed for the cases of Fig. 5(c) as well as Fig. 5(f), indicating that there is no bacteria growth uphill to the clean MG surface. Consequently, there is no induction property on the MG surface for DH5α. The microbiologic test results indicate that the Zr-based MG does not exhibit significant biotoxicity effect to *E. coli*. DH5α could also be cultured for more than 3 days such that the short-term biocompatibility of the Zr-based MG is confirmed. Results also indicate that the major factor in influencing the growth of DH5α is whether there is culture medium on the MG surface or not.

#### 4. Conclusions

Metallic glasses have been reported to be potential materials for future biomedical applications due to its unique metallic amorphous structure and material properties such as much higher strength and hardness. This paper reports the biocompatibility of various metallic glasses under in-vitro tests. Results show that the  $\text{Zr}_{61}\text{Cu}_{17.5}\text{Ni}_{10}\text{Al}_{7.5}\text{Si}_4$  metallic glass exhibits good corrosion resistance among the four MGs under study, showing no short-term biotoxicity. Although there is a small electrochemical response in the simulation body-fluid of Hank's solution, this metallic glass still shows its potential for biomedical application. The procedure developed in the present research provides a simple and rapid way for testing the biocompatibility of metallic glasses.

#### Acknowledgment

The financial supports from the National Science Council under the National Nano Project NSC 100-2120-M-110-004, and the NSYSU potential research group project are gratefully acknowledged.

#### References

- [1] J.W. Vahey, P.T. Simonian, E.U. Conrad III, Am. J. Orthop. 24 (1995) 319–324.
- [2] K. Arvidson, M. Cottlerfox, E. Hammarlund, U. Friberg, Scand. J. Dent. Res. 95 (1987) 356–363.
- [3] N. Jacobsen, A. Henstenpettersen, Eur. J. Orthod. 11 (1989) 254–264.
- [4] Z.L. Sun, J.C. Wataha, C.T. Hanks, J. Biomed. Mater. Res. 34 (1997) 29–37.
- [5] E. Kobayashi, S. Matsumoto, H. Doi, T. Yoneyama, H. Hamanaka, J. Biomed. Mater. Res. 29 (1995) 943–950.
- [6] E. Matykina, F. Monfort, A. Berkani, P. Skeldon, G.E. Thompson, J. Gough, J. Electrochem. Soc. 154 (2007) C279–C285.
- [7] M.H. Fathi, M. Salehi, A. Saatchi, V. Mortazavi, S.B. Moosavi, Dent. Mater. 19 (2003) 188–198.
- [8] P. Locci, C. Lilli, L. Marinucci, M. Calvitti, S. Belcastro, S. Bellocchio, N. Staffolani, M. Guerra, E. Becchetti, J. Biomed. Mater. Res. 53 (2000) 560–567.

- [9] D. Granchi, E. Cenni, G. Ciapetti, L. Savarino, S. Stea, S. Gamberini, A. Gori, A. Pizzoferrato, *J. Mater. Sci. Mater. Med.* 9 (1998) 31–37.
- [10] M.D. Demetriou, A. Wiest, D.C. Hofmann, W.L. Johnson, B. Han, N. Wolfson, G.Y. Wang, P.K. Liaw, *JOM* 62 (2010) 83–91.
- [11] J.R. Scully, A. Gebert, J.H. Payer, *J. Mater. Res.* 22 (2007) 302–313.
- [12] M.L. Morrison, R.A. Buchanan, R.V. Leon, C.T. Liu, B.A. Green, P.K. Liaw, J.A. Horton, *J. Biomed. Mater. Res. A* 74 (2005) 430–438.
- [13] A. Inoue, *Acta Mater.* 48 (2000) 279–306.
- [14] J. Schroers, *Adv. Mater.* 22 (2010) 1566–1597.
- [15] A. Inoue, T. Zhang, T. Masumoto, *Mater. Trans., JIM* 36 (1995) 391–398.
- [16] B. Zberg, P.J. Uggowitzer, J.F. Löffler, *Nat. Mater.* 8 (2009) 887–891.
- [17] L. Huang, Z. Cao, H.M. Meyer, P.K. Liaw, E. Garlea, J.R. Dunlap, T. Zhang, W. He, *Acta Biomater.* 7 (2011) 395–405.
- [18] Y.B. Wang, H.F. Li, Y.F. Zheng, M. Li, *Mater. Sci. Eng. C* 32 (2012) 599–606.
- [19] L. Liu, C.L. Qiu, M. Sun, Q. Chen, K.C. Chan, G.K.H. Pang, *Mater. Sci. Eng. A* 193 (2007) 449–451.
- [20] X.N. Gu, N. Li, Y.F. Zheng, Liquan Ruan, *Mater. Sci. Eng. B* 176 (2001) 1778–1784.
- [21] S. Hiromoto, A.P. Tsai, M. Sumita, T. Hanawa, *Corros. Sci.* 42 (2000) 1651–1660.
- [22] A. Kawashima, K. Ohmura, Y. Yokoyama, A. Inoue, *Corros. Sci.* 53 (2011) 2778–2784.
- [23] P.T. Chiang, G.J. Chen, S.R. Jian, Y.H. Shih, J.S.C. Jang, C.H. Lai, *Fooyin J. Health Sci.* 2 (2010) 12–20.
- [24] P.T. Chiang, G.J. Chen, S.R. Jian, Y.H. Shih, *Mater. Technol.* 27 (2012) 107–109.